Octane number influence on combustion and performance parameters in a Dual-Mode Dual-Fuel engine

Antonio García*, Javier Monsalve-Serrano, David Villalta and Rafael Sari

CMT - Motores Térmicos, Universitat Politècnica de València, Camino de Vera s/n, 46022 Valencia, Spain

Fuel, Volume 258, 15 Dec 2019, 116140
https://doi.org/10.1016/j.fuel.2019.116140

Corresponding author (*):
Dr. Antonio García Martínez (angarma8@mot.upv.es)
Phone: +34 963876574
Fax: +34 963876574

Abstract

Low temperature combustion stands as a promising alternative to realize low soot and NOx emissions while achieving fuel consumption benefits compared to the conventional diesel combustion. Nonetheless, its applicability is limited to narrow zones inside the engine map, reducing the potential benefits on a real driving case. In this scenario, the use of dual-mode dual-fuel combustion stands as an alternative to cover engine conditions up to full load, avoiding the constraints of the fully premixed combustion whenever is needed. This combustion concept is strongly influenced by the characteristics of the fuels that are used to create the charge stratification during the engine operation. The current research aims to evaluate the influence of the low reactivity fuel octane number on the combustion process and the average performance and emissions results. Additionally, the best octane number was determined by means of a merit function evaluation. Octane values of 100, 92.5, 87.5, 85 and 80 were obtained by blending iso-octane and heptane. Their performance was assessed in a medium-duty multi-cylinder platform at different representative operating conditions. The results suggest that fuels with octane number lower than 92.5 have a low impact at low load conditions. However, as load is increased, the high reactivity of the low research octane number fuels leads to early combustion processes, demanding settings modifications to avoid the appearance of excessive pressure gradients. As a consequence of these modifications, the fuel consumption and soot emissions increase. In general, RONs from 92.5 to 87.5 are less penalized, presenting the best merit function values, and therefore being the best fuels to be used in the hardware under investigation.

Keywords

Dual fuel combustion; primary reference fuel; emissions; reactivity controlled compression ignition; RON influence, octane number

1. Introduction

Despite of the constant claims affirming that transportation powered by internal combustion engines should be replaced by alternative forms as electrification, no

effective changes are seen in the current transport scenario [1]. Moreover, considering future predictions, the internal combustion engine (ICE) will still remain as the major power source for vehicles [2]. This situation is further pronounced at medium and heavy-duty transportation vehicles, where the energy consumption per vehicle and the usage rate are considerable higher than those from light-duty passenger cars [3]. Independently on the case, the powertrain design is constrained by the different restrictions imposed by the emissions regulations that become stricter during the years [4][5]. Therefore, the original equipment manufacturers (OEM) must realize different solutions to achieve the regulation limits. In most of the cases, post-combustion strategies are used by external devices with particular objectives as reduce the NOx (selective catalytic reduction, lean NOx trap), soot (diesel particulate filter), hydrocarbons (HC) and carbon monoxide (CO) (diesel oxidation catalyst) [6]. Nonetheless, this strategy has negative consequences on the total fuel consumption of the vehicle and represents an additional increment on the vehicle cost [7][8][9].

The control of the in-cylinder emissions generation should allow to decrease the requirements imposed to the after treatment devices, allowing to minimize their working and fixed costs or, in the best of the cases, to exclude them. In this sense, exhaustive research has been done to obtain new combustion concepts able to achieve reductions on the final emissions while maintaining similar efficiency levels than those found with the conventional diesel combustion [10][11]. As result, several combustion concepts were developed. Among them, the low temperature combustion (LTC) concepts demonstrated potential to avoid the soot-NOx trade-off with high efficiency [12]. Some of the most relevant LTC strategies are the homogeneous charge compression ignition (HCCI) [13][14], partially premixed compression ignition combustion (PPCI) [15][16], partially premixed combustion (PPC) [17] and reactivity controlled compression ignition (RCCI) [18]. The last one has advantages over the other LTC strategies as the better control over the combustion process by tailoring the in-cylinder reactivity, which is done by varying the amount of the two injected fuels (one with low reactivity and other with high reactivity) [19][20]. Unfortunately, none of the proposed LTC modes are able to cover all the engine map due to the excessive pressure gradients that appear at high loads and the low combustion efficiency occurring at low load conditions. Therefore, these combustion concepts are still limited to moderate loads inside the engine map [21][22] [23].

To overcome the issues from the single-mode LTC operation, Benajes et. al [24][25] developed the dual-mode dual-fuel (DMDF) combustion concept. This concept is based on using different strategies depending on the engine load. Up to medium loads, a fully premixed combustion is used, that leads to emissions and efficiency benefits. As the engine load increases, the injection strategy is modified to obtain a second diffusive combustion stage, allowing to reach the required engine load with pressure gradients under the mechanical restrictions [26]. Nonetheless, as the combustion becomes more diffusive, higher soot and NOx emissions are produced. The transition zone between combustion modes are primarily function of the fuel characteristics and the hardware limits in providing enough air and exhaust gas recirculation (EGR) to the combustion process. Therefore, the optimization of the fuel properties is a key point when looking for improvements in LTC operation limits. In this sense, Liu et al. [27] investigated the impact of the octane number (ON) on the combustion and emissions of a HCCI engine.

As a result of this work, it was verified that the high octane fuels allowed to extend the upper load limit of the HCCI combustion operation. Nonetheless, the low load conditions were impaired, resulting in excessive amounts of HC and CO. Similar investigations were performed in RCCI combustion by using a mixture of ethanol and gasoline (E85). In this case, the addition of ethanol in the fuel allowed to achieve a higher octane number. In general, the use of this fuel allows to extend the RCCI operation to wider ranges. Nonetheless, the HC and CO emissions at low loads are increased, limiting the lower limit operation [28][29].

Regarding DMDF combustion, there are a reduced number of investigations addressing the impact of the octane number on the different combustion modes set during the engine operation. In a multi-mode combustion concept, the definition of the best octane number is not a straightforward task. The improvements achieved at low to medium load operation can be balanced by the negative effect on the partially premixed combustion found at high load. This non-linear behavior is even more pronounced considering a driving cycle, where the operating conditions have different weights (according to the time spent) on the final results. Therefore, the steady-state evaluation cannot guarantee a proper evaluation when different behaviors are verified according to each zone of the engine map.

This research intends to evaluate the impact of the low reactivity fuel octane number on the combustion process, performance and emissions of a DMDF multi-cylinder engine. N-heptane and iso-octane were blended to obtain fuels with different octane number: 100, 92.5, 87.5, 85 and 80. The fuels were evaluated at six different operating conditions comprehending low, medium and high load conditions, corresponding to the different combustion strategies found in the calibration map. To compare the suitability of the fuels to be used in this combustion concept, a dedicated methodology is developed. In particular, the results of eight steady-state operating points are used to estimate those that would be found over the worldwide harmonized vehicle cycle (WHVC). This methodology is referred to as eight-modes because of its analogy with the 13-modes used in the past to evaluate the new European driving cycle (NEDC). To evaluate the precision of the eight-modes methodology, the results are compared to those obtained with a GT-power model using the complete calibration map. Finally, the different fuels are evaluated in a merit function allowing to determine the research octane number (RON) value that results in the best merit function values.

2. Materials and methods

2.1. Engine characteristics

The experimental investigations were performed in a multi-cylinder platform from a medium-duty, four stroke, serial production 8L engine. The engine is equipped with an optimized piston for the combustion concept, result from previous investigations [30]. To allow the operation at high loads, the geometric compression ratio was reduced from 17.5:1 to 12.75:1 and the engine was equipped with a low pressure EGR system. Table 1 summarizes the main characteristics of the engine.

Table 1. Engine characteristics.

Engine Type	4 stroke, 4 valves, direct injection
Number of cylinders [-]	6
Displaced volume [cm^3]	7700
Stroke [mm]	135
Bore [mm]	110
Piston bowl geometry [-]	Bathtub
Compression ratio [-]	12.75:1
Rated power [kW]	235 @ 2100 rpm
Rated torque [Nm]	1200 @ 1050-1600 rpm

2.2. Test cell description

The details of the experimental facility used during the experiments are presented in Figure 1. The test cell includes the different measurement devices that allow to record simultaneously instantaneous values of pressure, temperature, exhaust emissions and fuel consumption as well as to control the engine operating condition and the injection settings. During the experiments, the engine load and speed were controlled by means of an AVL active dynamometer using the AVL Puma interface. Average pressure and temperatures were monitored before and after the turbine and compressor as well as at both low pressure and high pressure EGR lines. Instantaneous in-cylinder pressure signals were recorded at each of the six cylinders by means of piezoelectric pressure transducers. The pressure signals were crank angle related by a digital encoder with a resolution of 0.2 CAD and acquired by a NI PXIe 1071. Real time processing was applied on the signals to obtain instantaneous heat release traces and the respective combustion assessment by a LabView routine. The same routine was used to acquire the instantaneous signals while time averaged signals were recorded by AVL Puma. Additionally, the LabView interface allows to control the injection settings for both low reactivity fuel (LRF) and high reactivity fuel (HRF) and the low pressure (LP) EGR system. The LP EGR system includes an electric backpressure valve to regulate the pressure gradient, a cooler, filters and dryers for particulates and water. The amount of LP EGR was controlled by a set of fast actuated electric valves located near to the intake manifold, before the compressor.

A five-gas Horiba MEXA-7100 DEGR analyzer was used to measure the gaseous engine-out emissions. Smoke emissions were measured in filter smoke number (FSN) units using an AVL 415S smoke meter. Three consecutive measurements of 1 liter volume each with paper-saving mode off were took at each engine operating point [31].The accuracy of the main elements of the test cell is presented in Table 2.

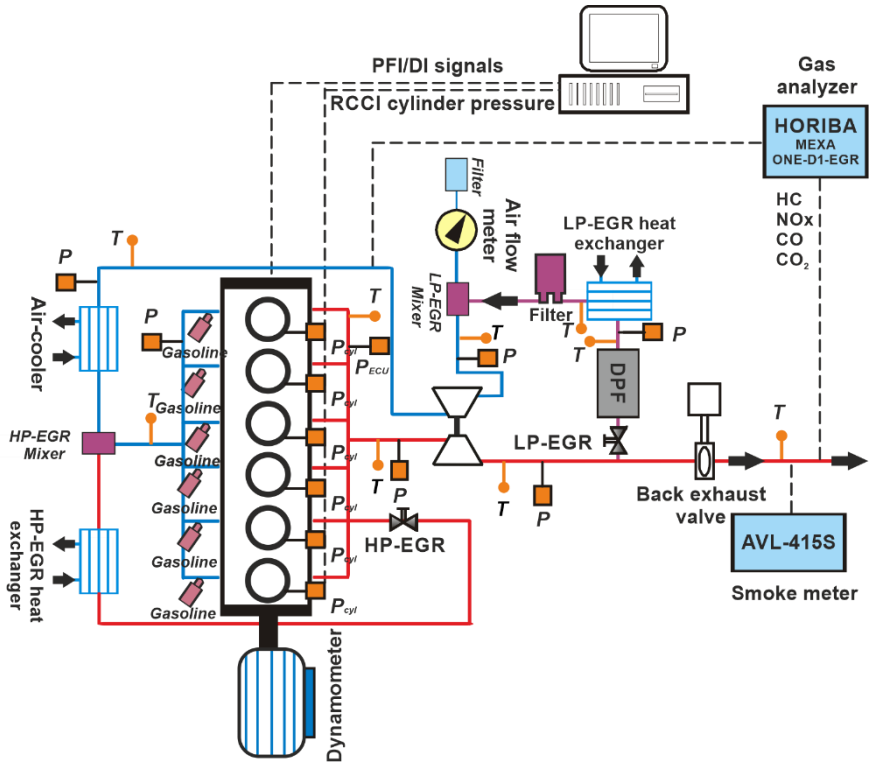

Figure 1. Test cell scheme.

Table 2. Accuracy of the instrumentation used in this work.

Variable measured	Device	Manufacturer / model	Accuracy
In-cylinder pressure	Piezoelectric transducer	Kistler / 6125C	±1.25 bar
Intake/exhaust pressure	Piezoresistive transducers	Kistler / 4045A	±25 mbar
Temperature in settling chambers and manifolds	Thermocouple	TC direct / type K	±2.5 °C
Crank angle, engine speed	Encoder	AVL / 364	±0.02 CAD
NOx, CO, HC, O_2, CO_2	Gas analyzer	HORIBA / MEXA 7100 DEGR	4%
FSN	Smoke meter	AVL / 415	±0.025 FSN
Gasoline/diesel fuel mass flow	Fuel balances	AVL / 733S	±0.2%
Air mass flow	Air flow meter	Elster / RVG G100	±0.1%

2.3. Fuels and injection systems characteristics

In this study, blends of n-heptane and isooctane were used to obtain low reactivity fuels with different RON values. In particular, a total of six different low reactivity fuels were tested, with RON values of 100, 92.5, 87.5, 85 and 80. Additionally, commercial gasoline was used as a reference of LRF during the tests. In terms of high reactivity fuel, EN 590 diesel was used in all the cases. The main characteristics of the different fuels are presented in Table 3.

Table 3. Physical and chemical properties of the fuels.

	EN 590 diesel	EN 228 gasoline	n-heptane	isooctane
Density [kg/m^3] (T= 15 °C)	842	720	645	658
Viscosity [mm^2/s] (T= 40 °C)	2.929	0.545		
RON [-]	-	95.6	0	100
MON [-]	-	85.7	0	100
Cetane number [-]	51	-	-	-
Lower heating value [MJ/kg]	42.50	42.4	44.57	44.43

The diesel fuel was injected into the cylinder using the stock common-rail fuel injection system, with a centrally located solenoid injector. The LRF was injected at the intake ports by means of port fuel injectors (PFI) located at the intake manifolds. All the injectors were handled through a DRIVVEN control system [40]. The direct injected (DI) and PFI fuel mass flows were measured using dedicated AVL 733S fuel balances. The main characteristics of the DI and PFI are depicted in Table 4.

Table 4. Characteristics of the direct and port fuel injectors.

Direct injector		Port fuel injector	
Actuation Type [-]	Solenoid	Injector Style [-]	Saturated
Steady flow rate @ 100 bar [cm^3/min]	1300	Steady flow rate @ 3 bar [cm^3/min]	980
Included spray angle [°]	150	Included Spray Angle [°]	30
Number of holes [-]	7	Injection Strategy [-]	single
Hole diameter [µm]	177	Start of Injection [CAD ATDC]	340
Maximum injection pressure [bar]	2500	Maximum injection pressure [bar]	5.5

2.4. Testing methodology

Six different operating conditions were evaluated during the experiments, which are presented in Figure 2. As it can be seen, the chosen operating conditions cover different zones of the calibration map. Operating conditions from 1 to 4 are examples of fully premixed combustion. Condition 5 is located at a partially premixed combustion whilst conditions 6 to 8 represents conditions where dual fuel diffusive combustion is used. Therefore, it is possible to assess the impact of the RON variation in different combustion strategies and engine loads.

At each condition, the calibration methodology described in [32] was applied in order to obtain the engine settings that allow to reach the minimum fuel consumption while maintaining the NOx and soot emissions below the levels imposed during the diesel-gasoline calibration. Therefore, using the same calibration methodology, the different fuels are comparable in their best calibration point. It is interesting to note that all the results shown in the manuscript have a coefficient of variation (COV) of the indicated mean effective pressure (IMEP) lower than 5%.

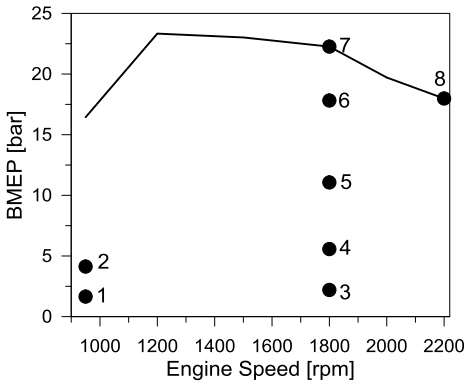

Figure 2. Operating conditions measured for evaluate the octane number impact.

2.5. Driving cycle approach

Steady-state results are useful to compare directly the performance of each fuel blend. However, this approach is not valid to define the best fuel for the current hardware because the time distribution along a driving cycle is not the same for each operating condition. To do this, a dedicated methodology was developed to extrapolate the transient behavior using steady-state results as input data. In particular, the results of eight steady-state operating points are used to estimate those that would be found over the WHVC. From now on, this methodology will be referred to as eight-modes because of its analogy with the 13-modes used in the past to evaluate the NEDC.

To validate the results obtained with the eight-modes method, a complete truck model was developed in GT-power (Figure 3), which has the same aerodynamic and geometrical characteristics than the truck which equips the 8L engine used in this work. The equations and assumptions used in this calculation were already discussed in previous work [33]. Additional information can be found in [34]. The vehicle model is fed with the complete steady-state calibration map. This map contains the results from 54 experimental tests at different engine speeds and loads, while the rest of the map is interpolated. In addition, the time-vehicle speed profile of the WHVC is also used as input for the model. Then, considering the vehicle dynamics, gear shifting strategy, etc., the final values of fuel consumption and emissions are computed. Finally, these results are compared to those obtained with the eight-modes method to evaluate its accuracy.

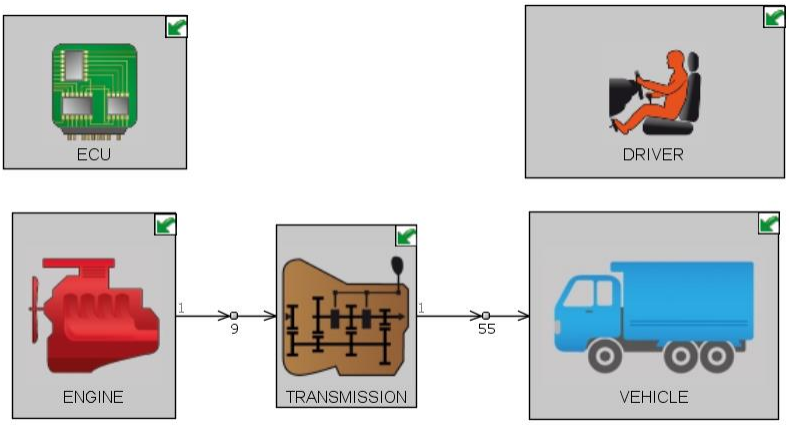

Figure 3. GT-Power vehicle model used as reference for the developed driving cycle approach.

To define the weight of each steady-state operating point in the final calculation using the eight-modes method, an adaptive approach is proposed. This approach considers an equivalent area in which the surrounding map values are similar to that experimentally measured. Starting from a small area around the experimental point, its size is increased in steps to embed the surrounding area in which the results have a deviation lower than 2%. To capture the trend of the variable represented on the map, three different strategies to increment the area were tested. The first one consists of incrementing the rectangle width according to a pre-determined step to capture trends that are invariant in engine speed. The second one is based on increments in the total height of the geometric element to capture trends that are invariant in engine load. Finally, the third strategy is a mixed mode, where an expansion factor is used allowing to expand the area in both directions to capture trends that are invariant in both engine speed and load. The three strategies are presented in Figure 4.

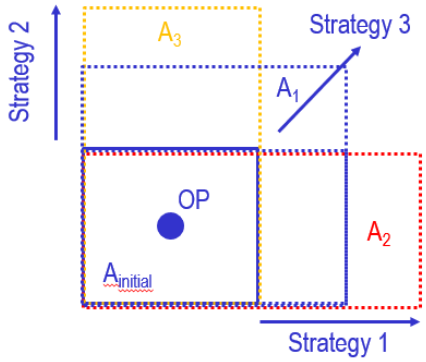

Figure 4. Different strategies employed to search the average area that represents the operating condition results

For each method, the initial area was steeply incremented and the average result of each step was compared to that from the experimental operating condition assuming a maximum deviation of 2%. Once this deviation was obtained, the iteration process stopped and the number of the driving cycle operating conditions covered by the final areas was counted (N_{Ai}). The operating points were obtained from the vehicle model. With the results from the area, the final results of the driving cycle could be obtained by the Equation 1. Note that the brake specific fuel consumption (BSFC) parameter can be replaced by any of the parameters that should be evaluated.

$$BSFC_{final} = \sum_{i=1}^{8} x_i \cdot BSFC_i$$

Where the ponderation factor x_i is obtained by

$$x_i = \frac{N_{Ai}}{\sum_{i=1}^{8} N_{Ai}}$$

Finally, the results obtained with the Equation 1 are compared to those obtained from GT-power for different engine maps and are presented in Table 5. As it can be seen, a proper agreement was obtained between both methodologies, validating the approach developed. Strategy 1 gives the best results for BSFC and soot while strategy 3 captures better the absolute values of NOx, HC and CO. This occurs due to the dependency of these variables to the engine speed and load. Therefore, the respective strategies were

used for the aforementioned properties in the development of the methodology. As it can be seen in Table 6, the accuracy of the eight-modes method is good enough to be able to define the best fuel for the current hardware. It is interesting to note that in spite of having an error of 25% for predicting the soot emissions, the values are ultra-low.

Table 5. Average results obtained from the different adaptive area strategies compared to the Gt-Power driving cycle.

	BSFC [g/kWh]	NOx [g/kWh]	CO [g/kWh]	HC [g/kWh]	Soot [g/kWh]	Total points	Points usage [%]
GT-power	261.00	0.36	12.63	3.33	0.003	11867.00	100
Strategy1	**253.51**	0.35	13.90	4.09	**0.004**	4522.00	38
Strategy2	287.85	0.35	13.45	4.27	0.006	7167.00	60.4
Strategy3	269.03	**0.36**	**12.59**	**3.53**	0.006	4963.00	41.8

Table 6. Accuracy of the eight-modes approach compared to GT-power model.

	BSFC [g/kWh]	NOx [g/kWh]	CO [g/kWh]	HC [g/kWh]	Soot [g/kWh]
GT-power	261.00	0.36	12.63	3.33	0.003
Eight-modes	**253.51**	**0.36**	**12.59**	**3.53**	**0.004**
Error [%]	2.9	0	0.32	5.6	25

2.6. Merit function

A merit function was defined to assess the potential of each fuel based on the results obtained with the eight-modes method. The merit function includes a limit imposed for each parameter and a weighting factor (F_i) to define the importance of each parameter on the merit function result. The emissions limits selected to calculate the merit function are those imposed by the EURO VI regulation (NOx_{limit}=0.46 g/kWh, CO_{limit}=4 g/kWh, HC_{limit}=0.16 g/kWh and $Soot_{limit}$=0.01 g/kWh). The value selected for the BSFC limit was that obtained from the vehicle running under conventional diesel combustion (CDC) operation along the WHVC ($BSFC_{limit}$=252 g/kWh). If the value obtained from the calculations in brackets is negative (i.e. the actual value is lower than the limit), the result of this operation is forced to be zero. Thus, the best fuel will be that which minimizes the merit function. It is interesting to note that the weighting factors must be selected in the order of magnitude of the variable, if not, the merit function result will be unbalanced. In this case, the weighting factors are F1=200, F2=0.2, F3=1, F4=0.1 and F5=0.02, so that the most important factors to be minimized are BSFC, NOx and soot because they weight double than the others.

$$MF_{PRFi} = F1 \cdot \left(\frac{BSFC_{final}}{BSFC_{limit}} - 1\right) + F2 \cdot \left(\frac{NOx_{final}}{NOx_{limit}} - 1\right) + F3 \cdot \left(\frac{Soot_{final}}{Soot_{limit}} - 1\right) + F4 \cdot \left(\frac{CO_{final}}{CO_{limit}} - 1\right) + F5 \cdot \left(\frac{HC_{final}}{HC_{limit}} - 1\right)$$

3. Results and discussion

This section presents the effect of the octane number on the performance and emissions of the DMDF combustion concept. To do this, the combustion process for five different fuels was studied at three operating conditions (25%@950rpm, 50%@1800rpm, 100%@2200rpm) by means of the heat release analysis. Later, the average values in terms of performance and engine-out emission will be discussed. Additionally, the limiting constraints that influence the PRF performance are also discussed to enlighten the challenges found in dual-fuel combustion when the RON is modified. Finally, the results from the merit function analysis are presented and discussed.

3.1. Combustion, performance and emission results

As literature suggests, the effect of the fuel RON on the combustion process varies depending on the engine speed and load. This effect can be more pronounced in the dual-fuel combustion process because two fuels of different reactivity are used, creating an environment where the reactivity stratification plays an important role on the combustion process. By this reason, the experimental tests to compare the fuels were performed at different engine speeds and loads, corresponding to different combustion modes inside the calibration map. This allows to understand the impact of the RON variation when the injection strategy and the ratio HRF and LRF injected is modified.

3.1.1. Low load, low speed operating condition

The final operation settings for each fuel, presented in Table 7, were achieved following the methodology discussed in section 2.4. As it can be seen, with exception of PRF 100, all the fuels present similar values in terms of air management, start of injection (SoI) and gasoline fraction (GF), while the injection pressure was kept constant for all the fuels. Regarding the PRF 100, the use of the same settings as those for the other fuels resulted in a too delayed combustion process as a consequence of the low reactivity of the fuel. To compensate that effect, the injection timing of the HRF had to be delayed in order to inject the HRF in a higher pressure and temperature ambient to initiate the combustion process. An advance of the HRF injection timing provoked an over dilution of the fuel and therefore a delayed CA50.

Table 7. Calibration settings obtained for the different PRFs for the condition of 25% of engine load at 950 rpm.

RON	P_{intake}	$P_{exhaust}$	Air mass	EGR	SoI	GF
[-]	[bar]	[bar]	[g/s]	[%]	[CAD bTDC]	[%]
100	1.08	1.16	37.23	44.15	15.00	38.83
92.5	1.08	1.16	35.19	41.45	19.00	47.31
87.5	1.07	1.15	35.94	44.08	19.00	46.70
85	1.08	1.16	36.33	43.23	19.00	47.49
80	1.08	1.16	35.25	44.50	19.00	46.09

Figure 5 shows the cycle averaged heat release profiles for each PRF. From this figure, it can be inferred that the RON variation has low effect on the combustion development at low engine loads. In general, excluding the RON 100, the heat release profile for the remaining RONs have similar shape and position. This result indicates that the

combustion process can be tailored from slightly changes in the engine settings to obtain a desired combustion phasing.

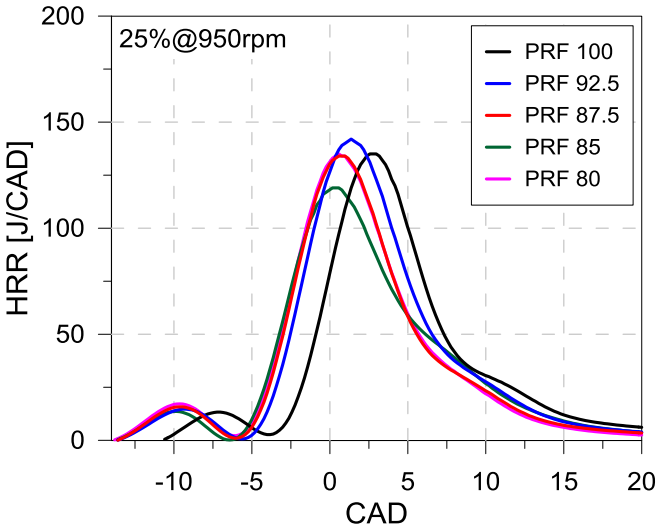

Figure 5. Heat release rates of the different evaluated PRFs for 950rpm of engine speed and 25% of engine load.

Figure 6(a) shows the main combustion metrics together with the break thermal efficiency (BTE) for the cases studied. The figure shows almost equal BTE for all the cases, which is explained by the similar combustion processes. In terms of combustion metrics, the figure shows similar CA50 for all the fuels with the exception of RON 100. As a general trend, the combustion duration increases with the RON, which is consequent to the lower in-cylinder mixture reactivity. Finally, the results show that the RON decrease promotes a slightly faster combustion development (CA90-CA10). From Figure 6(b), it can be seen that all the fuels allow fulfilling the calibration constrains in terms of NOx and soot emissions, with similar values of HC and CO. The lowest HC and CO emissions are obtained with PRF 92.5 due to its higher heat release rate (HRR) peak, which evidences greater in-cylinder temperatures.

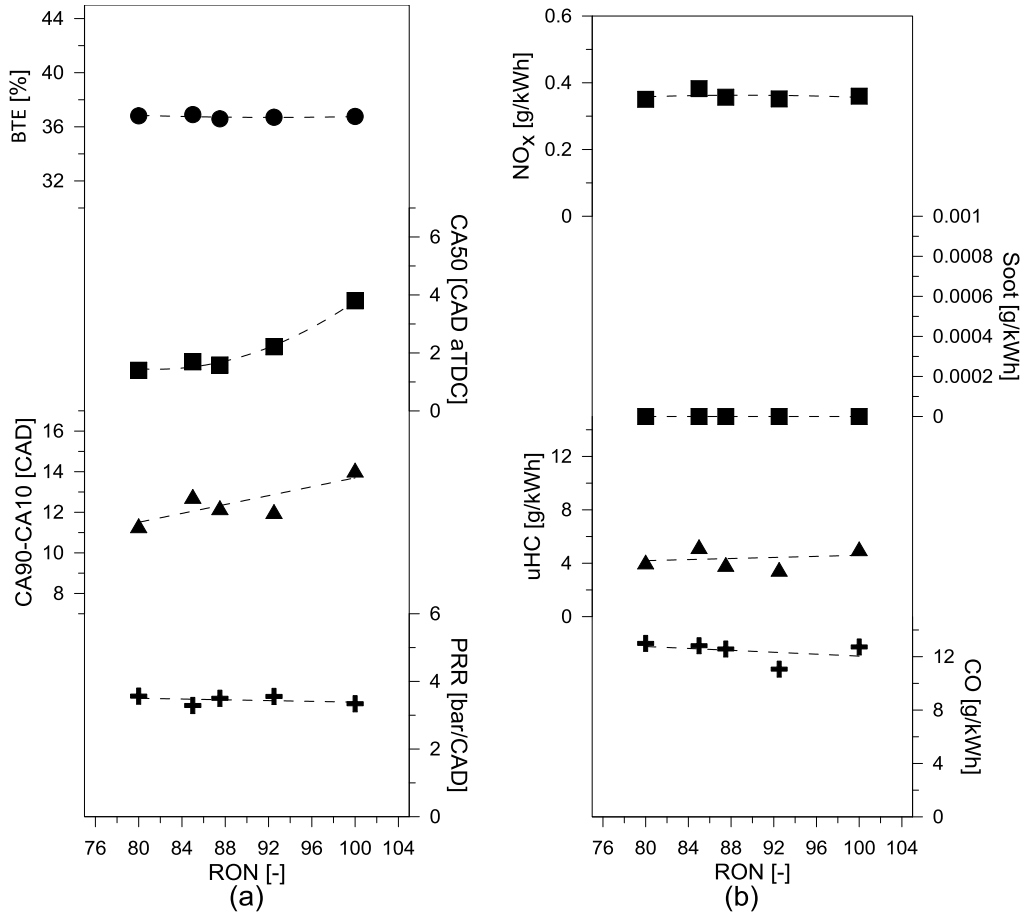

Figure 6. Main combustion metrics of the DMDF combustion strategy for different RONs at 25% and 950 rpm.

3.1.2. Medium load, moderate speed operating condition

The settings obtained for the different RONs at 50% load, 1800 rpm operating condition are presented Table 8. Their respective heat release rates are shown in Figure 7. The analysis of the optimal settings shown in Table 7 suggests that the variation of the fuel reactivity plays a major role on the combustion development at this condition. For octane numbers higher than 92, it was possible to maintain the injection timing, and the reactivity variation was balanced by increasing the EGR amounts whilst reducing the GF. This strategy allowed to maintain the pressure gradient values under the limiting constraints while fulfilling the EUVI normative for NOx and soot. As the RON was decreased from 92, the strategy had to be changed. This was justified by the impact of the higher EGR and lower GF in the soot production, exceeding the target constraints. In this case, the injection timing had to be shifted towards the top dead center (TDC), allowing to reduce the pressure gradient at the expense of decreasing the amount of premixed fuel. Therefore, it was possible to decrease the EGR rates as compared to the previous condition (PRF 92.5), achieving EUVI soot values. Finally, for RONs lower than 85, besides of the SoI modification, an additional decrease of the GF was required as a consequence of the mechanical constraints (pressure gradient). In this case, the inlet pressure was also increased to promote greater oxygen concentration and improve the soot oxidation. However, no fuel consumption benefits were achieved due to the increase of the pumping losses.

Table 8. Calibration settings obtained for the different PRFs for the condition of 50% of engine load at 1800 rpm.

RON	P_intake	P_exhaust	Air_mass	EGR	SoI	GF
[-]	[bar]	[bar]	[g/s]	[%]	[CAD bTDC]	[%]
100.00	2.11	2.44	145.08	38.98	50.00	88.97
92.50	2.10	2.73	114.30	46.31	50.00	78.81
87.50	1.99	2.44	112.71	43.00	40.00	79.34
85.00	2.16	2.61	120.58	44.57	30.00	77.05
80.00	2.21	2.66	129.20	43.12	24.00	69.81

Figure 7 illustrates the heat release rates obtained for the different RONs at this operating condition. These profiles represent the effect of the settings modification discussed previously. As it can be seen, the PRF 100 results in delayed combustion phasing as a consequence of the lower reactivity of this fuel. As the fuel RON is decreased, the start of combustion is advanced while the HRR peak is increased and the duration reduced. Nonetheless, as the RON is lowered from 87.5, the GF modifications results in higher combustion durations decreasing the HRR profile peak. Additionally, the highly advanced combustion process results in a high amount of energy released during the compression stroke. Nonetheless, as the combustion process occurs close to the TDC with a very short duration, the impact on the efficiency is not noticeable, as confirmed Figure 8(a).

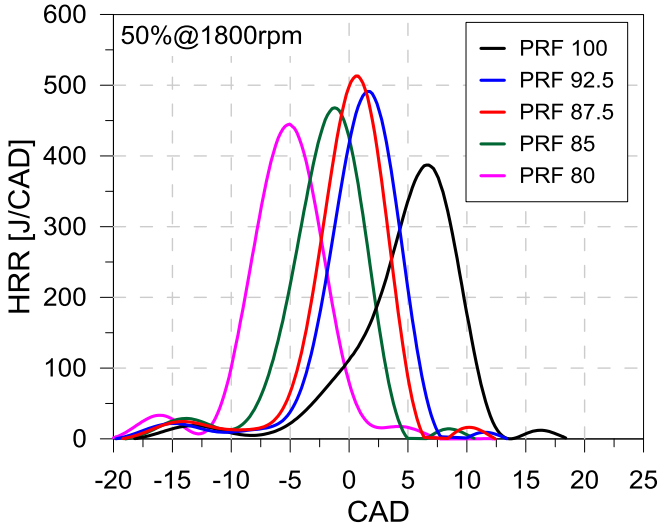

Figure 7. Heat release rates of the different evaluated PRFs for 1800rpm of engine speed and 50% of engine load.

As shown in Figure 8(a), the BTE values present a flat trend for almost all the RONs with the exception of PRF 100. One reason for the higher BTE with this fuel is the better phase achieved for the combustion process (CA50), which improves the fuel-to-work conversion efficiency. The ultra-low soot emissions achieved with this fuel is the result of an extended mixing time (from the end of injection up to the start of combustion) together with lower EGR amount and higher GF. The last two conditions promote the reduction of the fuel consumption. It is interesting to note that at this operating condition, the load increase started to be limited by the high pressure rise rates,

exceeding 10 bar/CAD for all conditions. The engine operation at pressure rise rate (PRR) levels higher than this limit can lead to mechanical fatigue and possible damage of the engine components.

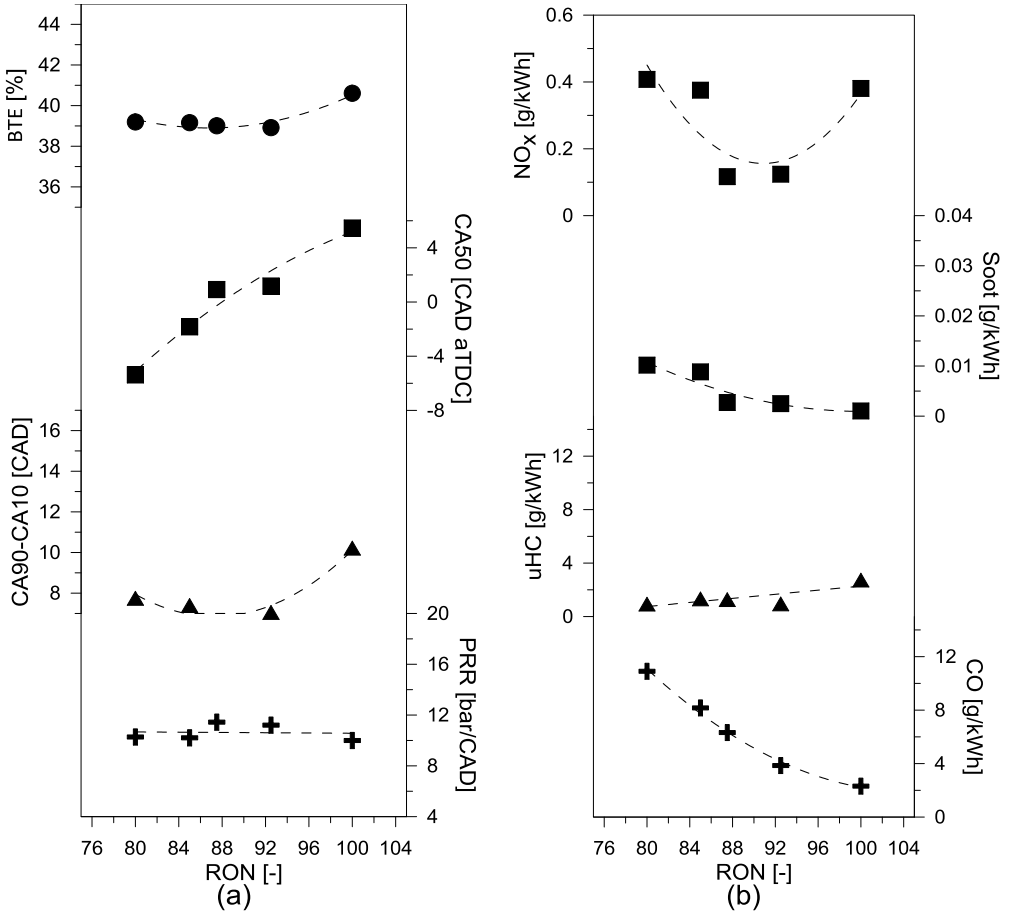

Figure 8. Main combustion metrics of the DMDF combustion strategy for different RONs at 50% and 1800 rpm.

Despite of the limitations for the low RONs, Figure 8 (b) shows that it was possible to achieve NOx and soot values inside the EUVI limits independently on the fuel used. The discussion about the problems verified with the soot emissions as the RON is decreased can be also verified in Figure 8 (b). It is possible to note that as the RON is decreased, the soot values are closer to those of the EUVI regulation. Even with the modification of the injection timing, GF and EGR values, it is difficult to reach the EUVI soot emissions levels. In addition, at RON 80, the NOx values are also at the limit of the regulation. In this case, three restrictions coexist at the same time: NOx, Soot and pressure gradient. From a calibration point of view, the strategies to reduce the pressure gradients and NOx will result in a soot increase and vice-versa. Therefore, it can be concluded that for the current hardware used in this research, RON 80 was the limiting octane number to obtain the calibration constraints desired. An additional decrease in the octane number will require a relaxation of the limits in soot or NOx. Regarding HC emissions, the trend is a function of the increase of the diesel amount inject. As the RON is decreased and so the GF, the higher amount of diesel promotes a better combustion process in terms of

combustion efficiency, reducing the final amount of unburned hydrocarbons. By contrast, the CO emissions are negatively impacted, increasing as the RON is decreased.

3.1.3. Full load, high speed operating condition

Finally, the full load operation at 2200 rpm is presented. The calibration strategy of this condition relies on a single diesel injection close to the TDC resulting in a dual-fuel diffusive combustion. The start of combustion is produced by the auto ignition of the low reactivity fuel while the engine load is regulated by the amount of HHR fuel injected. Therefore, the RON variation effect should be evidenced at the beginning of the combustion. The calibration constraints are relaxed to allow obtaining full load conditions. The maximum amount of NOx and Soot allowed at these conditions are 2 g/kWh and 2 FSN respectively. Table 9 summarizes the final calibration settings obtained for each one of the different fuel blends targeting the minimum fuel consumption while maintaining the NOx and soot emission levels under the limits. As it can be seen, the most expressive modification is verified in the GF values and the injection timing. In general, as the RON was decreased, lower GF values should be used with early injection timings to reduce the soot formation.

Table 9. Calibration settings obtained for the different PRFs for the condition of 100% of engine load at 2200 rpm.

RON	P_intake	P_exhaust	Air_mass	EGR	SoI	GF
[-]	[bar]	[bar]	[g/s]	[%]	[CAD bTDC]	[%]
100	2.79	3.33	276.35	19.90	10.00	41.15
92.5	2.61	3.10	263.34	19.15	11.00	38.82
87.5	2.59	3.05	260.34	20.72	12.00	38.95
85	2.83	3.38	273.17	21.56	13.00	38.65
80	2.72	3.19	265.66	20.18	12.00	36.71

The impact of the LRF RON can be observed at the HRR profiles presented in Figure 9. As it can be seen, for RON 100, the low reactivity of the fuel allowed to obtain a properly phased combustion process without exceeding the pressure gradient constraints. By contrast, as the RON is decreased, the premixed mixture reactivity increases, resulting in an early start of combustion. This means that the values of pressure and temperature closer to the diesel injection are higher, resulting in excessive pressure gradients once the diesel starts to burn. Therefore, the total amount of premixed mixture should be reduced to compensate this early combustion, being added to the HRR fuel, resulting in lower GF values. This allowed to obtain the same final IMEP for all the fuel blends. Nonetheless, the combustion duration is increased, penalizing the final efficiency of the cycle. It is interesting to note that the start of combustion is scaled with the reduction of the octane number, affirming that at this condition, the gasoline govern the first stage of the combustion development.

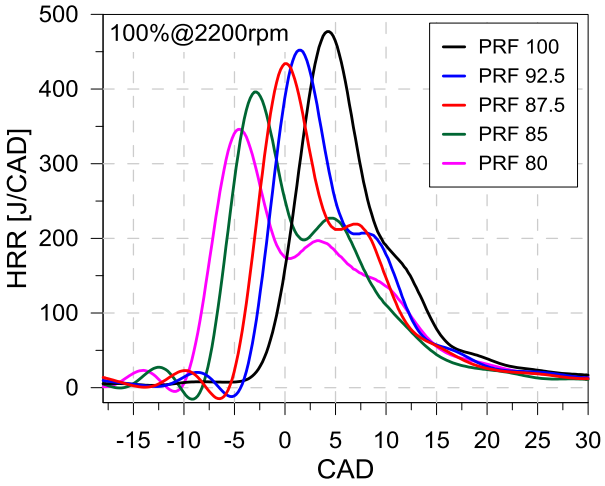

Figure 9. Heat release rates of the different evaluated PRFs for 2200rpm of engine speed and 100% of engine load.

Figure 10 presents the averages results in terms of performance and emissions parameters. As previously stated, the RON decrease required a reduction of the GF values, enlarging the combustion process. This impacts directly the final efficiency values as presented in Figure 10a. Additionally, the early start of combustion brings CA50 values closer to the TDC, resulting in higher amounts of energy released during the compression stroke, which also contributes to the reduction of the efficiency values.

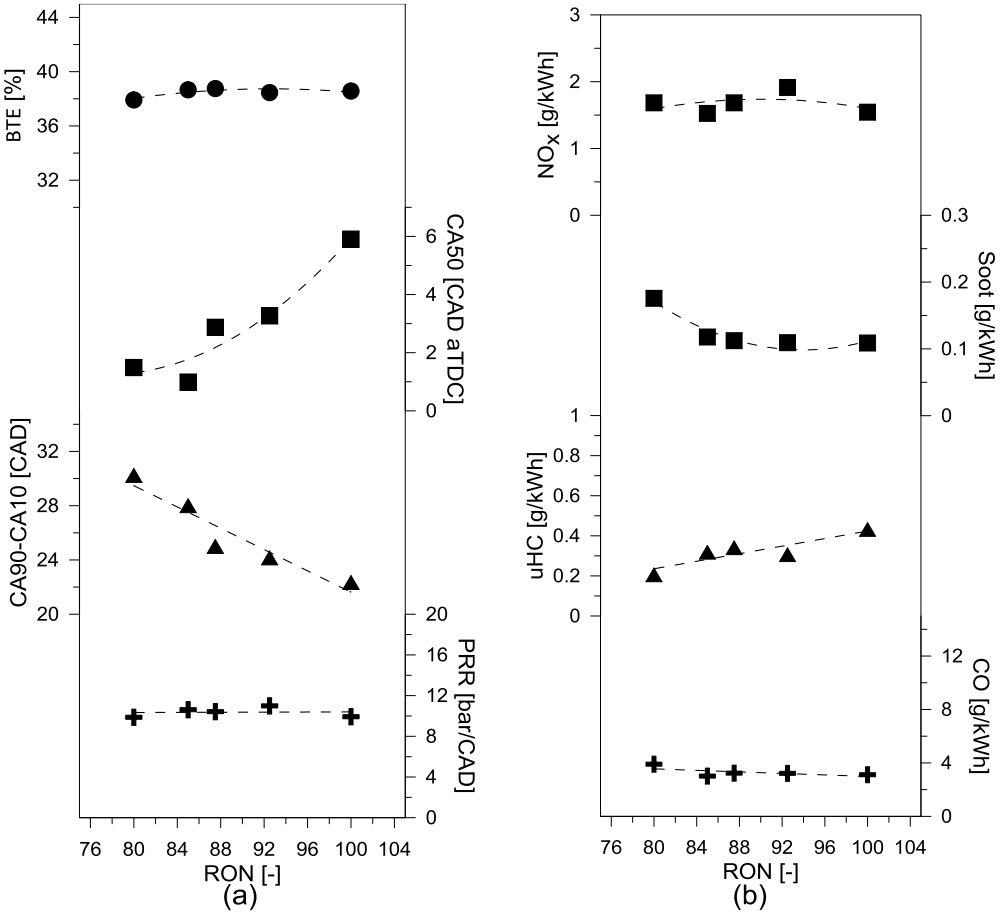

Figure 10. Main combustion metrics of the DMDF combustion strategy for different RONs at 100% and 2200 rpm.

Despite of this, it was possible to maintain the emissions values under the aimed constraints. A similar behavior than that verified at 50%@1800 rpm is observed at this condition for soot emissions. As higher amounts of diesel are used, the soot emissions tend to increase due to the more diffusive combustion process. By contrast, the uHC emissions are reduced.

Therefore, it can be concluded that the final effect of the RON on the combustion process is highly dependent of the engine load, which dictates the pressure and temperature values in which the combustion takes places. Additionally, the injection strategy and the GF values influences the reactivity stratification found at the early phases of the combustion development. In this sense, the influence of the RON can result in benefits for some conditions while can impair other. In order to be able to state the best RON to be used, the advantages and drawbacks realized must be weighted according to the importance of each operating condition.

3.2. Merit function

The results shown in the section 3.1 do not highlight which PRF is the best candidate to be used as low reactivity fuel for the dual-mode dual-fuel application. Since the emissions and fuel consumption do not follow the same trend as those found for the efficiency, the single analysis of the steady-state results is not enough. To estimate which PRF would provide the best results in a driving cycle, the methodology explained in the section 2.5 was applied. The results of the merit function analysis as a function of the different RONs evaluated are presented in Figure 11. As it can be seen, there is a decrease of the merit function values when the RON is decreased from 100 to 90. This is justified by the higher efficiency observed for low and medium load as the RON is decreased, with similar efficiencies at the high load condition. From RON 90, the MF starts to increase again as a consequence of the reduction of the brake efficiency at medium to high loads attributed to the longer combustion duration at these conditions.

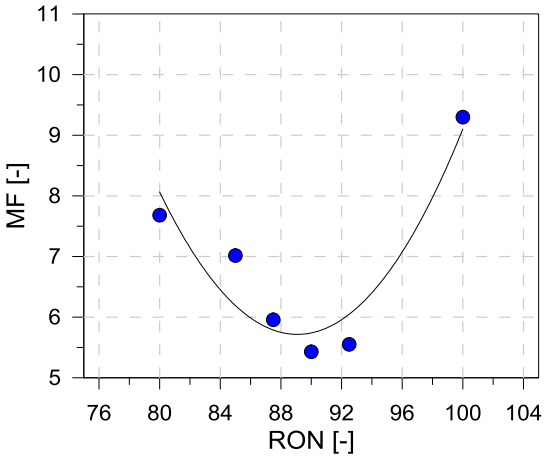

Figure 11. Merit function results for the different PRF fuels obtained thought the simplified driving cycle approach based on the 8 operating conditions measured.

Therefore, it can be stated that the optimal range of RON is from 87.5 to 95, where the minimum merit function values are found. This means that for this fuel RON range, the engine settings can be modified to obtain a proper calibration that have similar potential independently of the RON. Nonetheless, for values outside this range, the current hardware cannot deal with the required modifications to obtain a proper combustion

process, resulting in higher fuel consumption and higher emissions, thus increasing the final values of the merit function.

4. Conclusions

This paper evaluated the effect of RON variation on the performance and emission parameters of a multi-cylinder engine platform operating in DMDF combustion. Additionally, the optimal range of RON value was determined by means of a merit function approach based on an equivalent driving cycle.

From the first analysis, it was possible to verify that the effect of the RON variation is given in a different manner according to the combustion mode used. For low loads, the fully premixed combustion is weakly affected by the octane number. Therefore, slightly modifications of the engine settings are enough to provide similar combustion process independently of the RON. Nonetheless, when the engine load is increased to 50% at 1800 rpm, the high reactivity of the low octane fuels provides an early combustion process with high pressure gradients. In this sense, settings modifications are required to allow to reach the desired engine load fulfilling the calibration constraints. Finally, at 100% of engine load, the start of combustion is given by the auto ignition of the gasoline fuel, leading to excessive pressure gradients. In this case, the gasoline fraction values were decreased as the RON is decreased, leading to higher combustion durations and low efficiency values.

The global effect of these changes could be evaluated by applying the methodology developed based on the equivalent driving cycle. In this case, the local impact of the RON could be weighted according to each one of the operating conditions. RON values between 92.5 and 87.5 presented the minimum values of the merit function as a consequence of the small impact of the octane number on the fuel consumption as well as the emissions.

Acknowledgments

The authors thanks VOLVO Group Trucks Technology and ARAMCO Overseas Company for supporting this research. The authors also acknowledge FEDER and Spanish Ministerio de Economía y Competitividad for partially supporting this research through TRANCO project (TRA2017-87694-R) and the Universitat Politècnica de València for partially supporting this research through Convocatoria de ayudas a Primeros Proyectos de Investigación (PAID-06-18).

References

[1] Kalghatgi G. Is it really the end of internal combustion engines and petroleum in transport? Applied Energy, Volume 225, May 2018, Pages 965–974.
[2] U.S. Energy Information Administration (EIA). Annual Energy Outlook 2018 with projections to 2050. https://www.eia.gov/outlooks/aeo/pdf/AEO2018.pdf. [accessed 26 Oct 2018].
[3] U.S. Energy Information Administration (EIA). Annual Energy Outlook 2018 with projections to 2050. https://www.eia.gov/outlooks/aeo/pdf/AEO2018.pdf. [accessed 26 Oct 2018].

[4] The internal council of clean transportation. https:// www. theicct.org/ sites/ default/files/publications/ICCT_Euro6 VI_briefing_jun2016.pdf. [accessed 26 Oct 2018].
[5] Luján JM, Bermúdez V, Dolz V, Monsalve-Serrano J. An assessment of the real-world driving gaseous emissions from a Euro 6 light-duty diesel vehicle using a portable emissions measurement system (PEMS). Atmospheric Environment, Volume 174, Feb 2018, Pages 112-121.
[6] Gense N. L. J., Riemersma, Such C., Ntziachristos L. Euro VI technologies and costs for Heavy Duty vehicles: the expert panels summary of stakeholders responses. TNO Science and Industry, September 2006.
[7] Yamauchi T, Takatori Y, Fukuda K. Experimental and Numerical Analysis for a Urea-SCR Catalytic Converter. SAE Technical Paper 2016-01-0973. https://doi.org/10.4271/2016-01-0973.
[8] Singh N, Rutland C, Foster D, Narayanaswamy K, He Y. Investigation into Different DPF Regeneration Strategies Based on Fuel Economy Using Integrated System Simulation. SAE Technical Paper 2009-01-1275. https://doi.org/10.4271/2009-01-1275.
[9] Posada F., Chambliss S. and Blumberg K. Costs of emission reduction technologies for heavy-duty diesel vehicles". ICCT White paper, 2016.
[10] Reitz R. D., Duraisamy G. Review of high efficiency and clean reactivity controlled compression ignition (RCCI) combustion in internal combustion engines. Progress in Energy and Combustion Science. Volume 46, August 2014, Pages 12-71.
[11] Saxena S., Bedoya I. D. Fundamental phenomena affecting low temperature combustion and HCCI engines, high load limits and strategies for extending these limitsVolume 39, Issue 5, 2013, Pages 457-488, ISSN 0360-1285, https://doi.org/10.1016/j.pecs.2013.05.002.
[12] Benajes J, García A, Monsalve-Serrano J, Boronat V. Gaseous emissions and particle size distribution of dual-mode dual-fuel diesel-gasoline concept from low to full load. Applied Thermal Engineering, Volume 120, 25 Jun 2017, Pages 138-149.
[13] Epping K., Aceves S., Bechtold R. and Dec J. The Potential of HCCI Combustion for High Efficiency and Low Emissions. SAE Technical Paper 2002-01-1923, 2002, https://doi.org/10.4271/2002-01-1923.
[14] Yang Y, Dec J, Dronniou N, Sjöberg M. Tailoring HCCI heat-release rates with partial fuel stratification: Comparison of two-stage and single-stage-ignition fuels. Proceedings of the Combustion Institute, Volume 33 (2), pp. 3047-3055, 2011.
[15] Benajes Calvo, JV.; García Martínez, A.; Doménech Llopis, V.; Durret, R. An investigation of partially premixed compression ignition combustion using gasoline and spark assistance. Applied Thermal Engineering. 52(2):468-477. doi:10.1016/j.applthermaleng.2012.12.025.
[16] Benajes J, Molina S, García A, Monsalve-Serrano J, Durrett R. Performance and engine-out emissions evaluation of the double injection strategy applied to the gasoline partially premixed compression ignition spark assisted combustion concept. Applied Energy, Volume 134, 2014, Pages 90-101, ISSN 0306-2619,https://doi.org/10.1016/j.apenergy.2014.08.008.
[17] Noehre C., Andersson M., Johansson B. and Hultqvist, A. Characterization of Partially Premixed Combustion. SAE Technical Paper 2006-01-3412, 2006, https://doi.org/10.4271/2006-01-3412.

[18] Molina S, García A, Monsalve-Serrano J, Estepa D. Miller cycle for improved efficiency, load range and emissions in a heavy-duty engine running under reactivity controlled compression ignition combustion. Applied Thermal Engineering, 136, Pages 161-168, 2018.

[19] Olmeda P, García A, Monsalve-Serrano J, Lago Sari R. Experimental investigation on RCCI heat transfer in a light-duty diesel engine with different fuels: Comparison versus conventional diesel combustion. Applied Thermal Engineering, 144, Pages 424-436, 2018.

[20] Benajes J, García A, Monsalve-Serrano J, Lago Sari R. Fuel consumption and engine-out emissions estimations of a light-duty engine running in dual-mode RCCI/CDC with different fuels and driving cycles. Energy, 157, Pages 19-30, 2018.

[21] Benajes J, García A, Monsalve-Serrano J, Villalta D. Exploring the limits of the reactivity controlled compression ignition combustion concept in a light-duty diesel engine and the influence of the direct-injected fuel properties. Energy Conversion and Management, Volume 157, February 2018, Pages 277-287.

[22] Benajes J, García A, Monsalve-Serrano J, Balloul I, Pradel G. Evaluating the reactivity controlled compression ignition operating range limits in a high-compression ratio medium-duty diesel engine fueled with biodiesel and ethanol. International Journal of Engine Research, Volume 18 (1-2), Pages 66-80, 2017.

[23] Splitter D, Wissink M, Kokjohn S and Reitz R. Effect of Compression Ratio and Piston Geometry on RCCI Load Limits and Efficiency. SAE Technical paper, 2012-01-0383

[24] Benajes J, García A, Monsalve-Serrano J, Boronat V. Achieving clean and efficient engine operation up to full load by combining optimized RCCI and dual-fuel diesel-gasoline combustion strategies. Energy Conversion and Management, Volume 136, 15 March 2017, Pages 142-151.

[25] García A, Monsalve-Serrano J, Rückert Roso V, Santos Martins M. Evaluating the emissions and performance of two dual-mode RCCI combustion strategies under the World Harmonized Vehicle Cycle (WHVC). Energy Conversion and Management, Volume 149, 1 Oct 2017, Pages 263-274

[26] J. Benajes, A. García, J. Monsalve-Serrano, V. Boronat, Dual-fuel combustion for future clean and efficient compression ignition engines, Appl. Sci. 7 (1) (2017) 36.

[27] Liu H., Yao M., Zhang B., Zheng Z. Effects of Inlet Pressure and Octane Numbers on Combustion and Emissions of a Homogeneous Charge Compression Ignition (HCCI) Engine.,Energy & Fuels 2008 22 (4), 2207-2215DOI: 10.1021/ef800197

[28] Benajes J, García A, Monsalve-Serrano J, Villalta D. Benefits of E85 versus gasoline as low reactivity fuel for an automotive diesel engine operating in reactivity controlled compression ignition combustion mode. Energy Conversion and Management, Volume 159, March 2018, Pages 85-95.

[29] Splitter D, Wissink M, Kokjohn S and Reitz R. Effect of E85 on RCCI Performance and Emissions on a Multi-Cylinder Light-Duty Diesel Engine. SAE Technical Papers 2012-01-0383, doi:10.4271/2012-01-0383

[30] Benajes J, García A, Pastor JM, Monsalve-Serrano J. Effects of piston bowl geometry on Reactivity Controlled Compression Ignition heat transfer and combustion losses at different engine loads. Energy, Volume 98, March 2016, Pages 64-77.

[31] AVL manufacturer manual. Smoke value measurement with the filter-papermethod. Application notes. June 2005 AT1007E, Rev. 02. Web:<https://www.avl.com/documents/10138/885893/Application+Notes
[32] Benajes J, Pastor J. V., García A., Monsalve-Serrano J. The potential of RCCI concept to meet EURO VI NOx limitation and ultra-low soot emissions in a heavy-duty engine over the whole engine map, Fuel, Volume 159, 2015, Pages 952-961, ISSN 0016-2361, https://doi.org/10.1016/j.fuel.2015.07.064.
[33] Benajes J.; García A.; Monsalve-Serrano J.; Sari R. Fuel consumption and engine-out emissions estimations of a light-duty engine running in dual-mode RCCI/CDC with different fuels and driving cycles. Energy, 2018, 157, 19-30
[34] GT-Suite. Engine performance application manual, 2016.

Abbreviations

ATDC: After Top Dead Center

BSFC: Brake Specific Fuel Consumption

CAD: Crank Angle Degree

CDC: Conventional Diesel Combustion

CO: Carbon Monoxide

COV: Coefficient Of Variation

DI: Direct Injection

DMDF: Dual Mode Dual Fuel

EGR: Exhaust Gas Recirculation

FSN: Filter Smoke Number

GF: Gasoline Fraction

HC: Hydro Carbons

HCCI: Homogeneous Charge Compression Ignition

HRR: Heat Release Rate

HRF: High Reactivity Fuel

ICE: Internal Combustion Engine

IMEP: Indicated Mean Effective Pressure

LP: Low Pressure

LRF: Low Reactivity Fuel

LTC: Low Temperature Combustion

MON: Motor Octane Number

NEDC: New European Driving Cycle

NOx: Nitrogen Oxides

OEM: Original Equipment Manufacturer

PFI: Port Fuel Injection

PPC: Partially Premixed Combustion

PPCI: Partially Premixed Compression Ignition

PRR: Pressure Rise Rate

RCCI: Reactivity Controlled Compression Ignition

RON: Research Octane Number

TDC: Top Dead Center

WHVC: Worldwide Harmonized Vehicle Cycle